

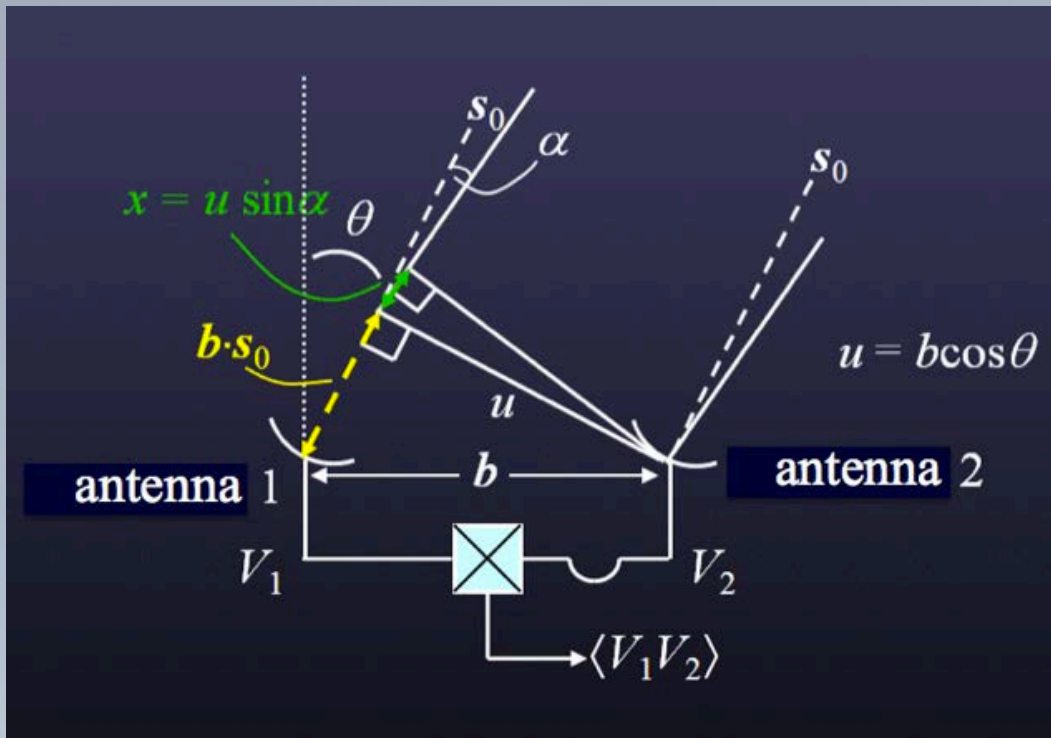


# Overview

Synthesis Imaging,  
Deconvolution, & Self-calibration

T. S. Bastian (NRAO)

# The fundamental element: a pair of antennas



$$\langle V_1 V_2 \rangle = \langle \iint V_1(l, m) V_2(l, m) dl dm \rangle$$

$$\langle V_1 V_2 \rangle = \iint \langle V_1(l, m) V_2(l, m) \rangle dl dm$$

$$x = u \sin \alpha = ul \quad V_2 = V_1 e^{2\pi i (ul)}$$

$$\langle V_1 V_2 \rangle = \iint \langle V_1(l, m)^2 \rangle e^{2\pi i (ul + vm)} dl dm.$$

$$\langle V_1 V_2 \rangle \propto \iint I(l, m) e^{2\pi i (ul + vm)} dl dm$$

$$V(u, v) = \iint A(l, m) I(l, m) e^{-2\pi i (ul + vm)} dl dm.$$

Using the van Cittert-Zernike theorem under fairly relaxed assumptions (the most important being a small FOV), the radio brightness distribution and the visibility function are related through a **Fourier transform**.

$$\mathcal{V}(u, v) = \iint I(l, m) e^{2\pi i(ul + vm)} dl dm$$

$$I(l, m) = \iint \mathcal{V}(u, v) e^{-2\pi i(ul + vm)} du dv$$

The use of this relationship in practice involves a number of practicalities.



Modern arrays exploit the Fourier transform relationship between  $V(u,v)$  and  $I(l,m)$  to perform **Fourier synthesis** imaging.

An array of  $N$  antennas yields  $N(N-1)/2$  pairs of antennas. An antenna baseline with coordinates  $(u_k, v_k)$  samples the visibility function at  $V(u_k, v_k)$ . Moreover, since the sky brightness is **real**, the visibility function is **Hermitian** and  $V(u_k, v_k) = V^*(-u_k, -v_k)$ . The sampling function can then be expressed

$$B(u, v) = \sum_{k=1}^{2M} \delta(u - u_k, v - v_k).$$

This is just the auto-correlation function of the antenna distribution.

$$I_V^D(l, m) = \iint \mathcal{V}(u, v) B(u, v) e^{-2\pi i(ul + vm)} du dv$$

Expressed another way (ignoring additive noise):

$$I^D(l, m) = FT^{-1}\{B(u, v)V(u, v)\}.$$

$$I^D(l, m) = b(l, m) * I(l, m)A(l, m).$$

where  $b(l, m)$  is “synthesized beam”, “dirty beam”, or “point spread function”, the inverse Fourier transform of the sampling function  $B(u, v)$ ; and  $I^D(l, m)$  is the so-called “dirty map”, the convolution of the dirty beam with the “true” brightness distribution  $I(l, m)$  multiplied by the primary beam  $A(l, m)$ .

In order to recover the “true” brightness distribution one must deconvolve the dirty beam or PSF  $b(l, m)$  from the dirty map  $I^D(l, m)$ .

# Image formation & deconvolution

To make an image, we must represent the dirty map and beam in discrete (pixel) form; i.e., we must evaluate  $I^D(l,m)$  on a uniform grid. One way is to compute the **Discrete Fourier Transform** on an  $N \times N$  grid:

$$I^D(l,m) = \frac{1}{M} \sum_{k=1}^M V'(u_k, v_k) e^{2\pi i (ul+vm)}$$

Far more commonly, because  $M$  is large and because the number of desired pixels is large, the **Fast Fourier Transform** is used. However, the data must be sampled on a uniform grid to use the FFT.

This is done by convolving the data with a smoothing function and resampling onto a uniform grid.



# Image formation & deconvolution

It is very useful to be able to **weight** the sampling function to, e.g., optimize angular resolution or sensitivity to extended emission. Write the weighted sampling a function

$$W(u, v) = \sum_{k=1}^M T_k D_k \delta(u - u_k, v - v_k)$$

where  $T_k$  is a (Gaussian) taper and  $D_k$  is a weight based on the uv sampling density. We then have

$$V^W(u, v) = \sum_{k=1}^M T_k D_k \delta(u - u_k, v - v_k) V'(u, v)$$

which allows control over sidelobe weighting and noise. **Natural** and **uniform** weighting are commonly used, as is a more optimum weighting scheme called “**robust**” or **Briggs** weighting.

# Image formation & deconvolution

The deconvolution problem can be expressed simply as

$$I^D = B * I + n$$

where  $n$  has been separated out as additive noise. The measurement equation is ill-posed. Implicit in the principle solution  $I^D$  is the assumption that all visibilities that were not measured are zero.

Let  $z$  be a brightness distribution that contains only those spatial frequencies that were unmeasured. Then if  $I$  is a solution to the measurement equation, so is  $I + \alpha z$  (since  $B * z = 0$ ) !

Deconvolution can be thought of as that process by which the unmeasured visibilities are estimated.



# Image formation & deconvolution

Two classes of deconvolution algorithm are commonly employed in radio astronomy:

**CLEAN** is a simple shift-and-subtract algorithm with many variants [Hogbom, Clark, MSC, MTMS – see <https://casa.nrao.edu/casadocs/casa-5.1.0/synthesis-imaging/deconvolution-algorithms>] designed to speed it up, stabilize its performance, or to handle extended or complex brightness distributions.

**MEM** and related algorithms maximize the configurational entropy of the model image, usually subject to known constraints such as the noise and total flux.

Other deconvolution schemes: SVD, ASP, Pixon, algebraic

# Self-calibration

We have ignored some of the messy realities related to the calibration of visibility data. Brushing certain complexities under the rug, one can relate the observed visibility  $V'_{ij}$  to the “true” visibility  $V_{ij}$  on antenna baseline  $ij$  through

$$V'_{ij}(t) = g_i(t)g_j^*(t)V_{ij}(t) + \epsilon_{ij}(t)$$

The approach to calibration commonly employed is to regularly observe one or more sources with known properties to solve for the complex gains  $g_i(t)$  and to transfer them to the source data through interpolation.

This is problematic for ALMA because the atmosphere, which introduces phase and amplitude variations to the effective gain, can change between calibrations.

# Self-calibration

The water vapor radiometers (WVR) on each antenna mitigate phase variations introduced by the atmosphere for non-solar sources. Self-calibration is also used to correct gain phase and amplitude. Solar observations must rely solely on self-calibration.

The basic idea is this: we allow the antenna gain to be a free parameter that we solve for by minimizing the difference between the data and a model of the source. An interferometer with many antennas produces many visibility measurements compared with the number gains to be deduced:  $\sim(N-2)/2$ . It is a highly over-constrained problem for large-N arrays like ALMA.



# Self-calibration

The procedure can be summarized as a minimization of the following quantity by adjusting the gains  $g_i, g_j$

$$S = \sum_k \sum_{i,j} w_{ij}(t_k) |V'_{ij}(t_k) - g_i(t_k)g_j^*(t_k)V^m_{ij}(t_k)|^2$$

It is worth rewriting this as

$$S = \sum_k \sum_{i,j} w_{ij}(t_k) |V^m_{ij}(t_k)|^2 |X_{ij}(t_k) - g_i(t_k)g_j^*(t_k)|^2$$

$$X_{ij} = \frac{V'_{ij}(t)}{V^m_{ij}(t)}$$

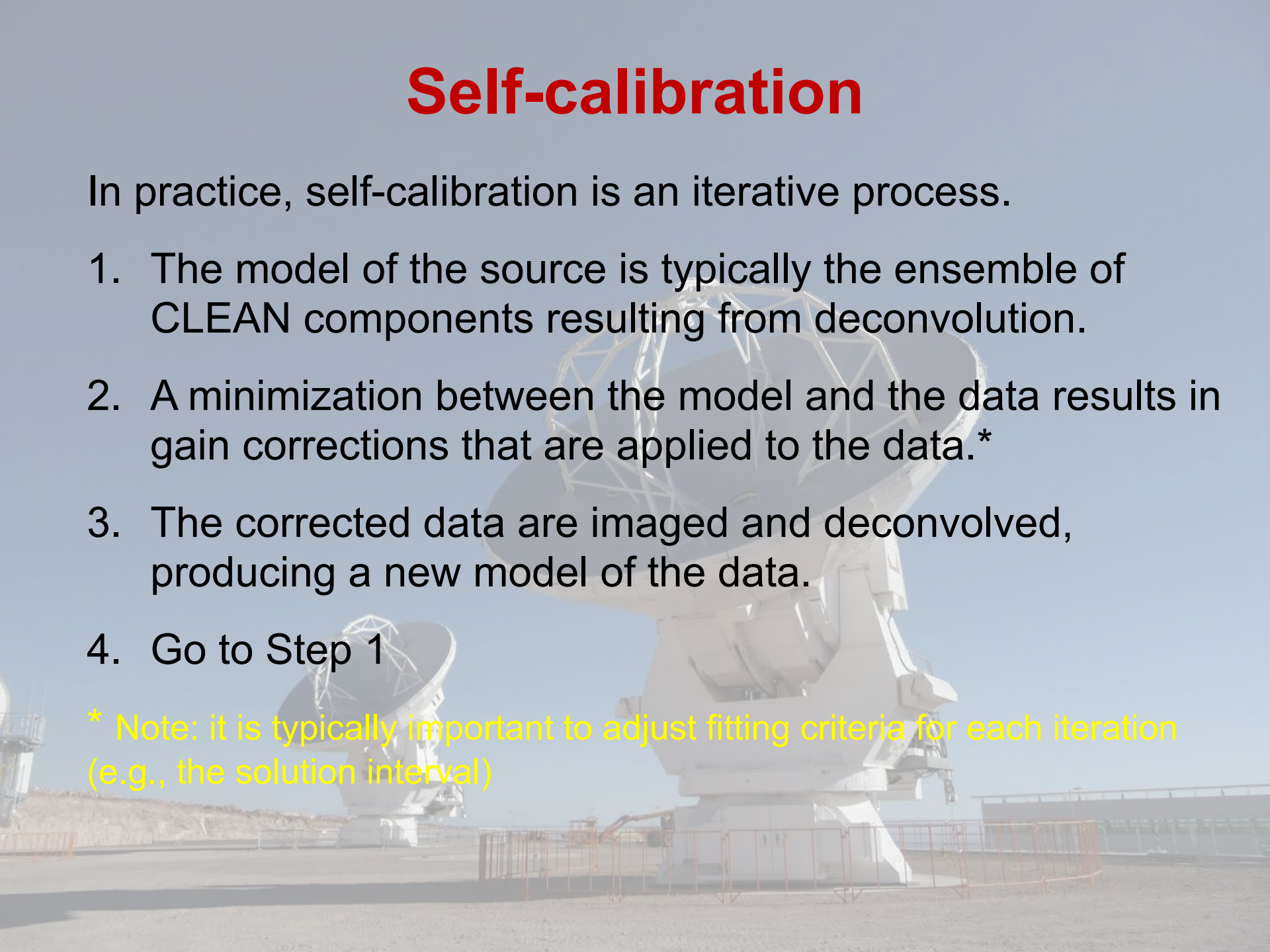
In effect, changing the source into a pseudo-point source for which the complex gains (or the phase part only) are determined in much the same way as for a regular calibrator source.

# Self-calibration

In practice, self-calibration is an iterative process.

1. The model of the source is typically the ensemble of CLEAN components resulting from deconvolution.
2. A minimization between the model and the data results in gain corrections that are applied to the data.\*
3. The corrected data are imaged and deconvolved, producing a new model of the data.
4. Go to Step 1

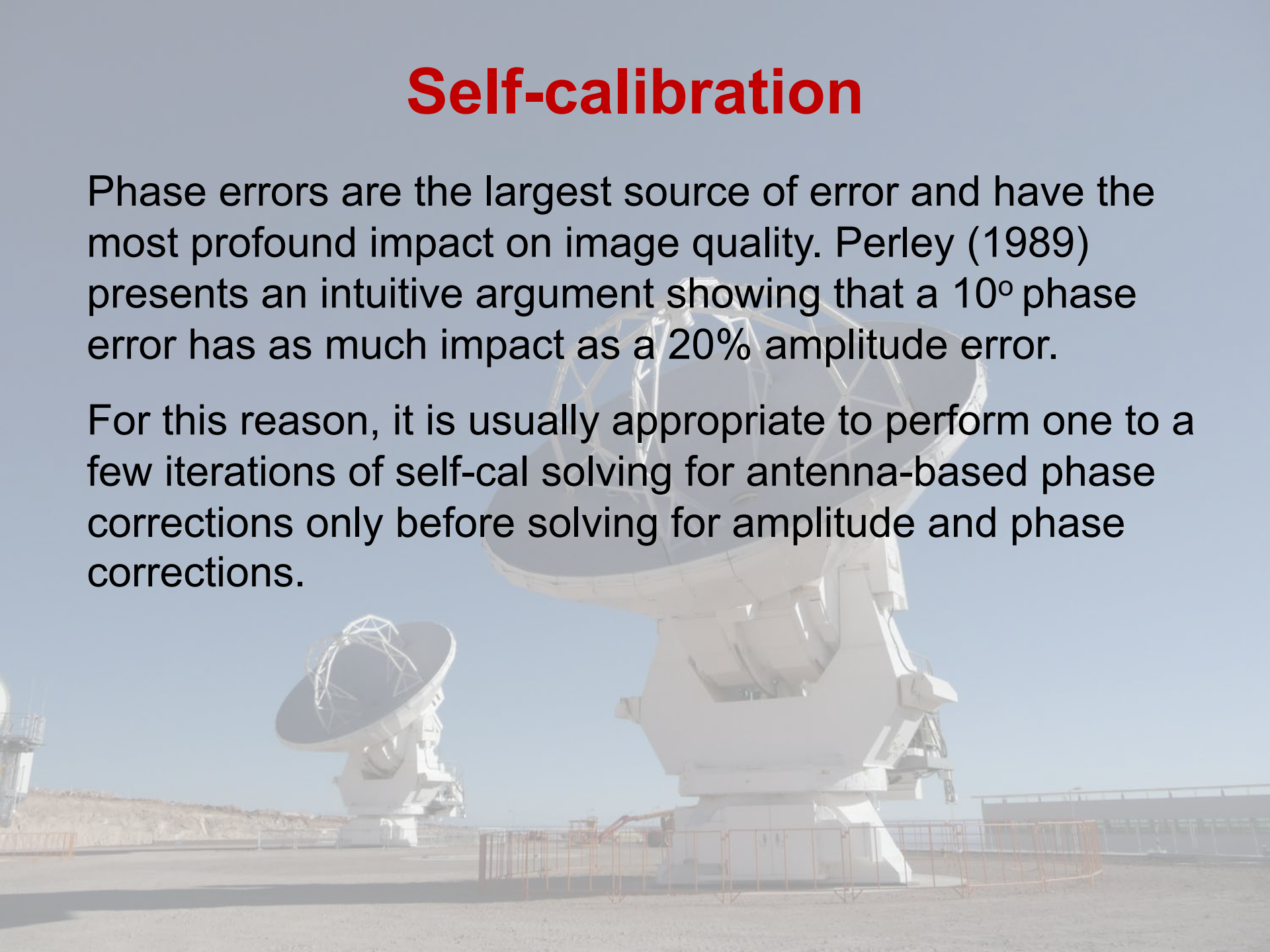
\* Note: it is typically important to adjust fitting criteria for each iteration (e.g., the solution interval)



# Self-calibration

Phase errors are the largest source of error and have the most profound impact on image quality. Perley (1989) presents an intuitive argument showing that a  $10^\circ$  phase error has as much impact as a 20% amplitude error.

For this reason, it is usually appropriate to perform one to a few iterations of self-cal solving for antenna-based phase corrections only before solving for amplitude and phase corrections.



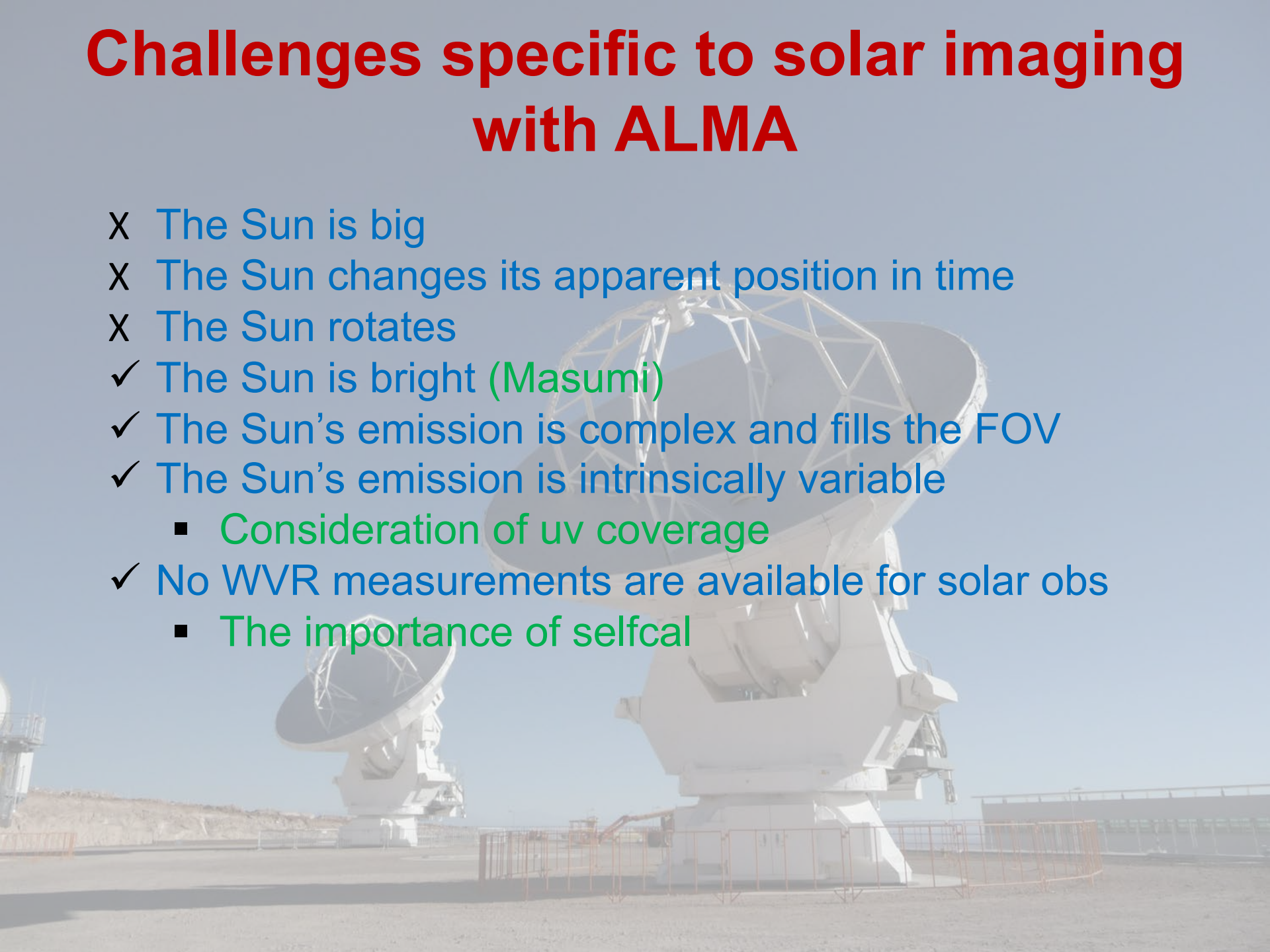


# Challenges specific to solar imaging with ALMA

1. **The Sun is big** – much larger than the ALMA FOV in any band, requiring TP fast mapping, mosaicing
2. **The Sun changes its apparent position in time** – requiring the instrument to track its apparent motion
3. **The Sun rotates** – requiring the instrument to track its differential rotation, too
4. **The Sun is bright** – necessitating changes to the hardware, software, and calibration procedures
5. **The Sun's emission is complex and fills the FOV** – thereby requiring excellent uv coverage
6. **The Sun's emission is intrinsically variable** – requiring excellent snapshot uv coverage as well
7. **No WVR measurements are available for solar obs**

# Challenges specific to solar imaging with ALMA

- X The Sun is big
- X The Sun changes its apparent position in time
- X The Sun rotates
- ✓ The Sun is bright (Masumi)
- ✓ The Sun's emission is complex and fills the FOV
- ✓ The Sun's emission is intrinsically variable
  - Consideration of uv coverage
- ✓ No WVR measurements are available for solar obs
  - The importance of selfcal



# uv coverage

ALMA is comprised of the 12m array (50 antennas), the ACA (10 7m antennas), and 4 total power antennas.

	Band	3	4	5	6	7	8	9	10	
	Frequency (GHz)	100	150	185	230	345	460	650	870	
Config.		<i>Briggs</i>	<i>natural</i>							
7-m	$\theta_{res}$ (arcsec)	(11.6)	12.5	8.35	6.77	5.45	3.63	2.72	1.93	1.44
	$\theta_{MRS}$ (arcsec)	(66.0)	66.7	44.5	36.1	29.0	19.3	14.5	10.3	7.67
C-1	$\theta_{res}$ (arcsec)	3.38	(3.16)	2.25	1.83	1.47	0.98	0.735	0.52	0.389
	$\theta_{MRS}$ (arcsec)	28.5	(25.8)	19.0	15.4	12.4	8.25	6.19	4.38	3.27
C-2	$\theta_{res}$ (arcsec)	2.30	(3.00)	1.53	1.24	0.999	0.666	0.499	0.353	0.264
	$\theta_{MRS}$ (arcsec)	22.6	(24.8)	15.0	12.2	9.81	6.54	4.9	3.47	2.59
C-3	$\theta_{res}$ (arcsec)	1.42	(2.03)	0.943	0.765	0.615	0.41	0.308	0.218	0.163
	$\theta_{MRS}$ (arcsec)	16.2	(18.8)	10.8	8.73	7.02	4.68	3.51	2.48	1.86
C-4	$\theta_{res}$ (arcsec)	0.918	(1.29)	0.612	0.496	0.399	0.266	0.2	0.141	0.106
	$\theta_{MRS}$ (arcsec)	11.2	(13.6)	7.5	6.08	4.89	3.26	2.44	1.73	1.29

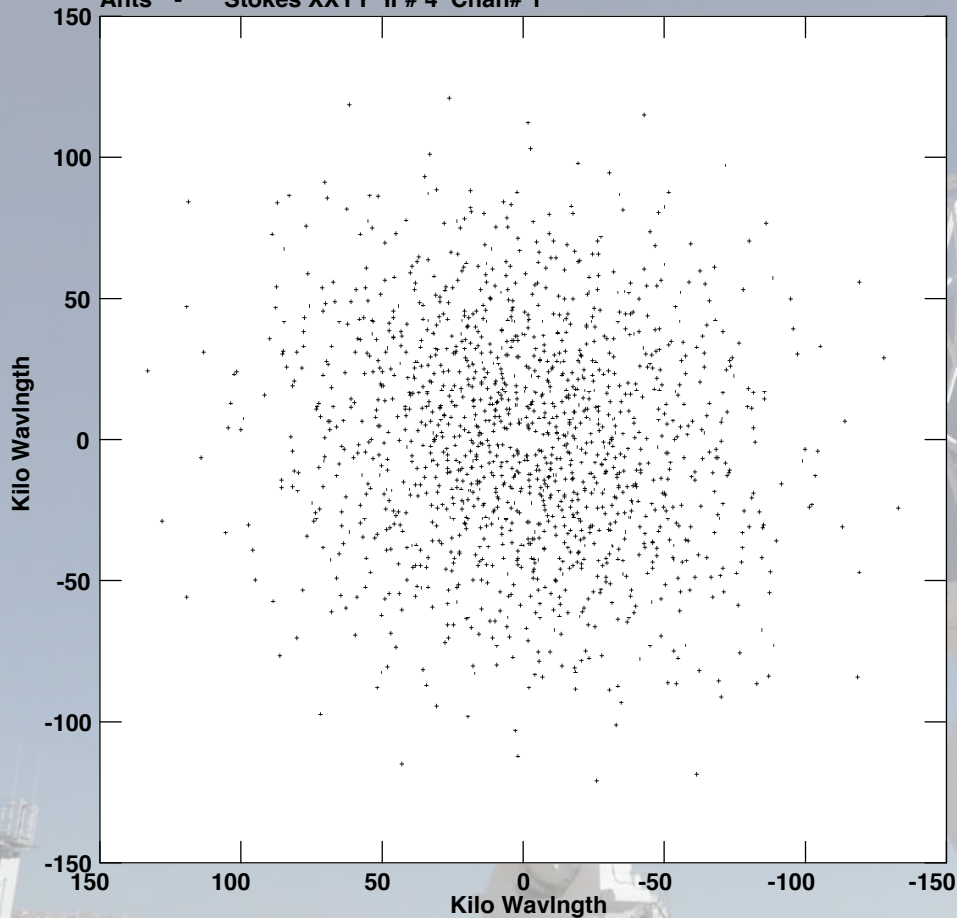
The angular resolution is determined by the longest baseline:  $\theta_{res} \sim \lambda / b_{max}$  while the “maximum recoverable scale” is  $\theta_{MRS} \sim \lambda / b_5$

Configuration	7-m	C-1	C-2	C43-3	C-4
Minimum baseline (m)	8.7	14.6	14.6	14.6	14.6
5th percentile or L05 (m)	9.1	21.4	27.0	37.6	54.1
80th percentile or L80 (m)	30.7	107.1	143.8	235.4	369.2
Maximum baseline (m)	45.0	160.7	313.7	500.2	783.5

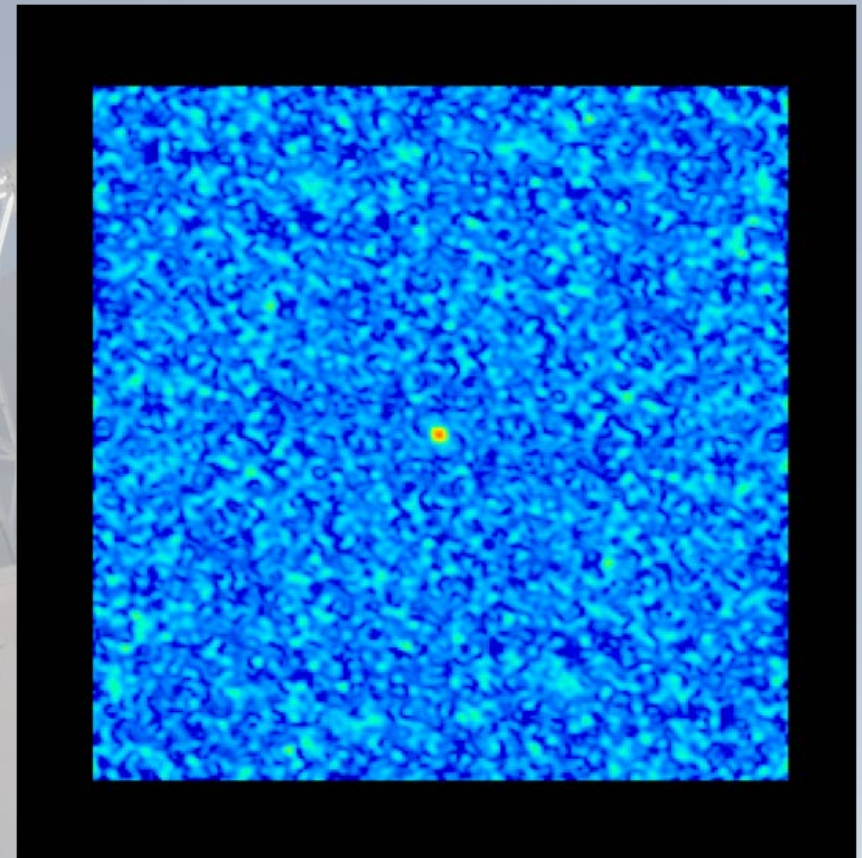


# ALMA Band 3

Plot file version 1 created 24-FEB-2020 13:26:37  
V vs U for SUN 3 MM.UVR12.1 Source:Sun\_10  
Ants \* \_ \* Stokes XXYY IF# 4 Chan# 1



From 0/17:25:00 to 0/17:25:02

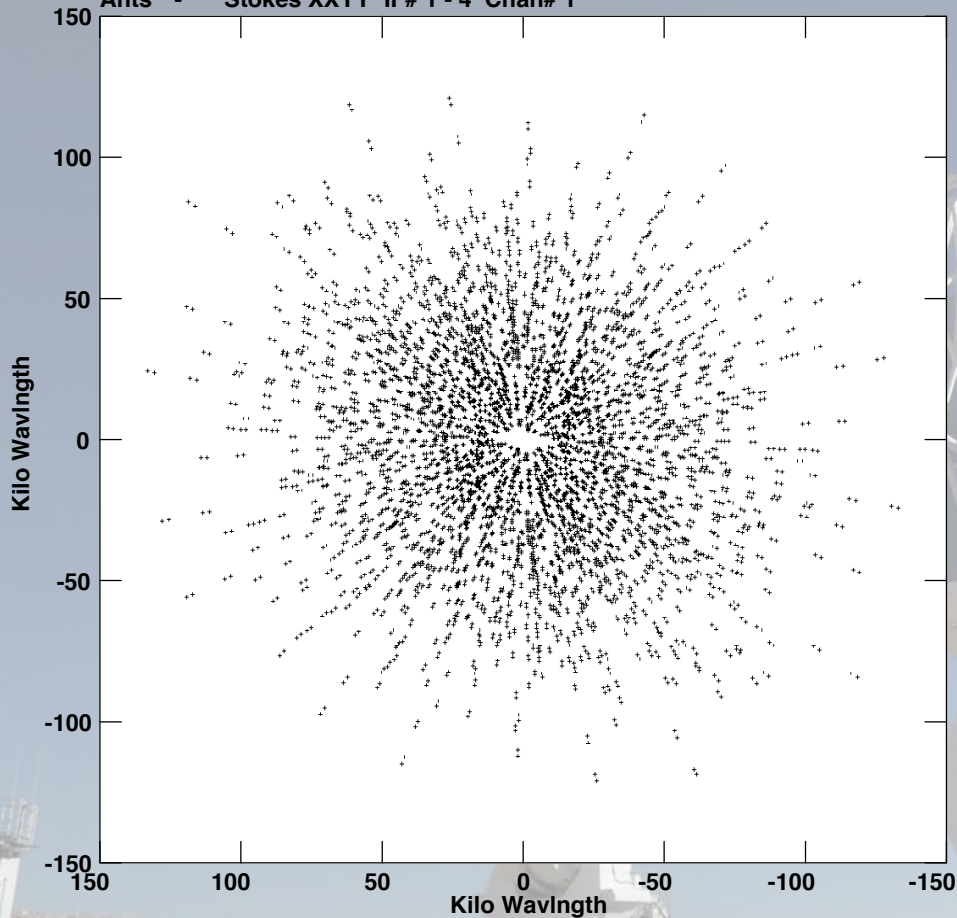


2 s snapshot, spw 3, 12m array

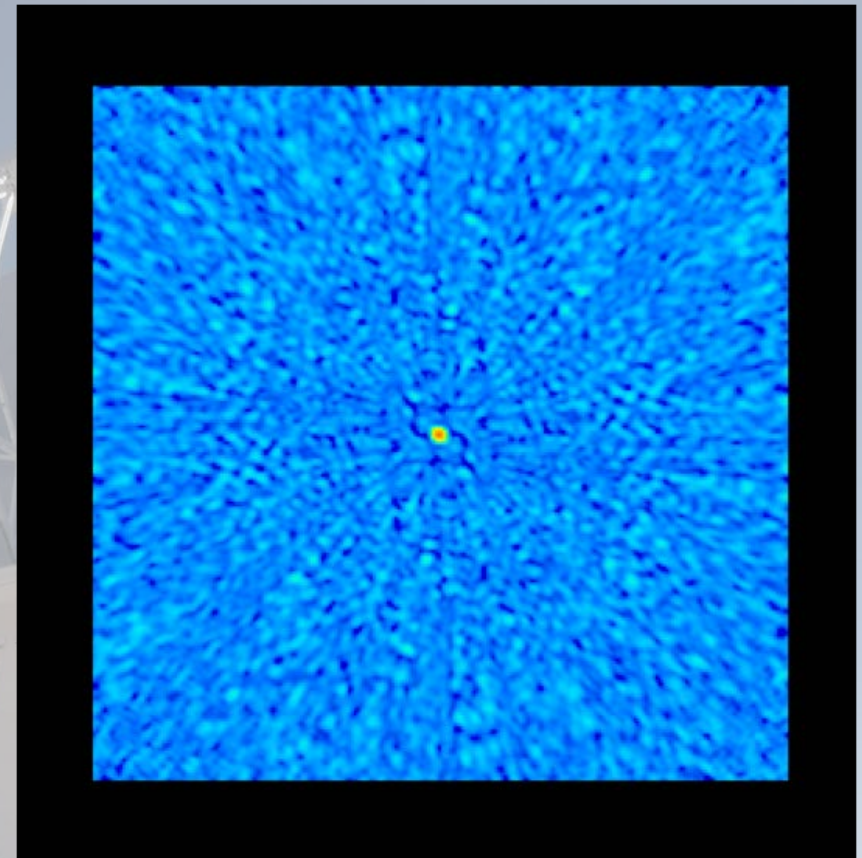
“Dirty beam”: rms  $\sim$  2.6%  
(far sidelobes)

# ALMA Band 3

Plot file version 2 created 24-FEB-2020 13:26:43  
V vs U for SUN 3 MM.UVR12.1 Source:Sun\_10  
Ants \* - \* Stokes XXYY IF# 1 - 4 Chan# 1



From 0/17:25:00 to 0/17:25:02



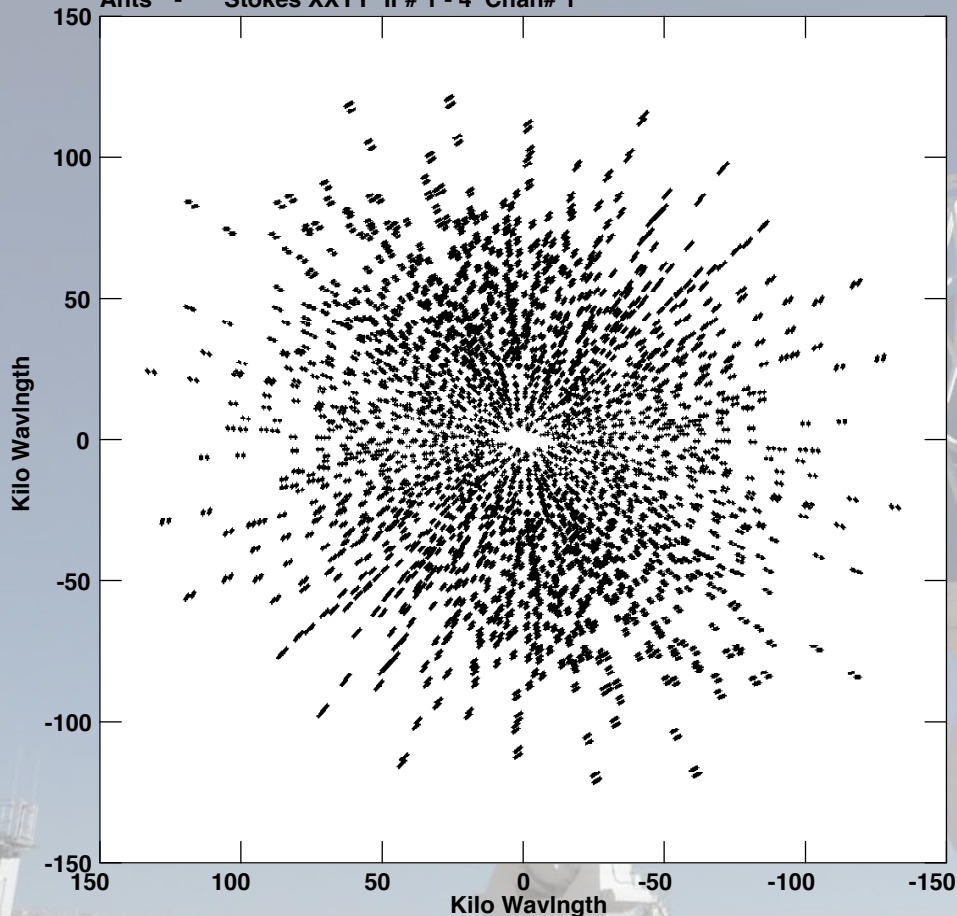
2 s snapshot, spw 0~3, 12m array

“Dirty beam”: rms ~ 1.6%

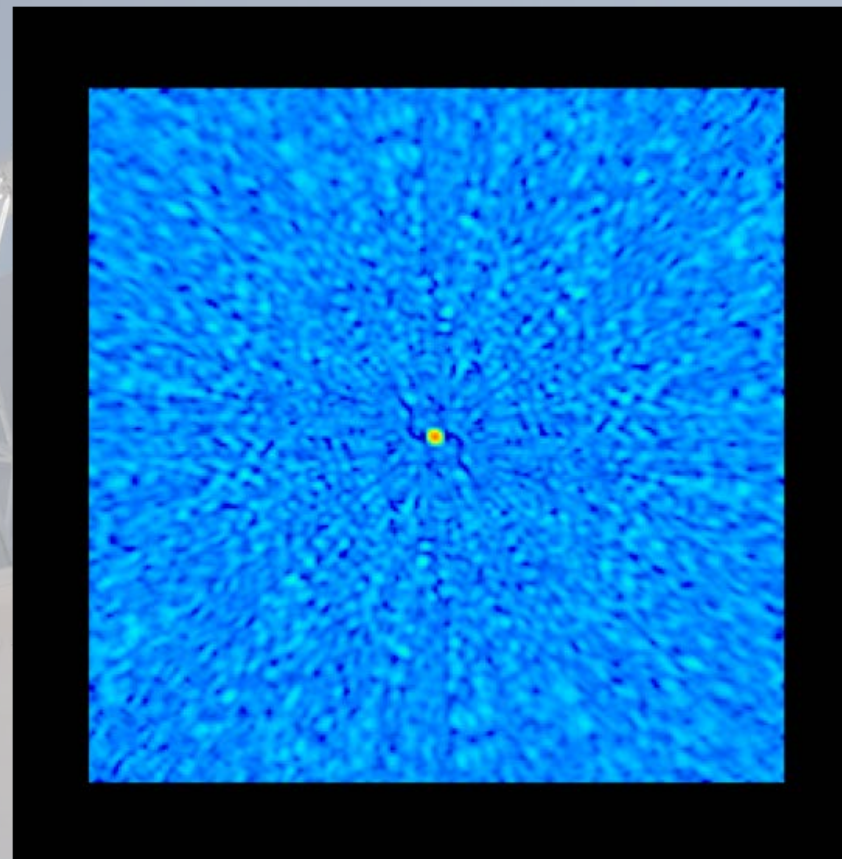


# ALMA Band 3

Plot file version 3 created 24-FEB-2020 13:27:02  
V vs U for SUN 3 MM.UVR12.1 Source:Sun\_10  
Ants \* - \* Stokes XXYY IF# 1 - 4 Chan# 1



From 0/00:00:00 to 0/17:32:00



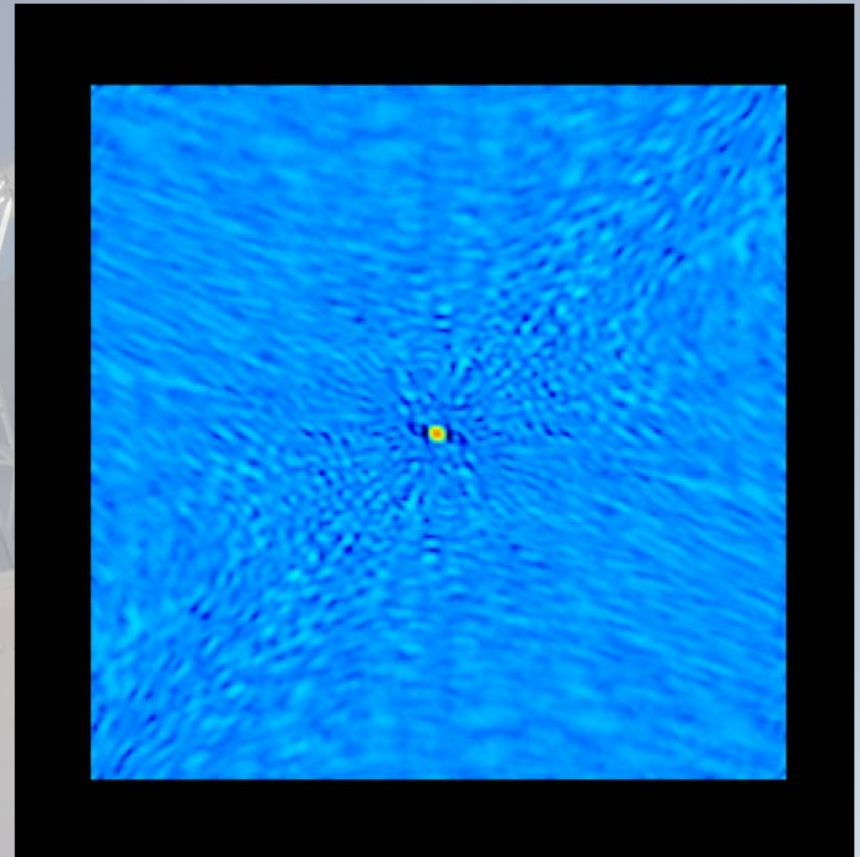
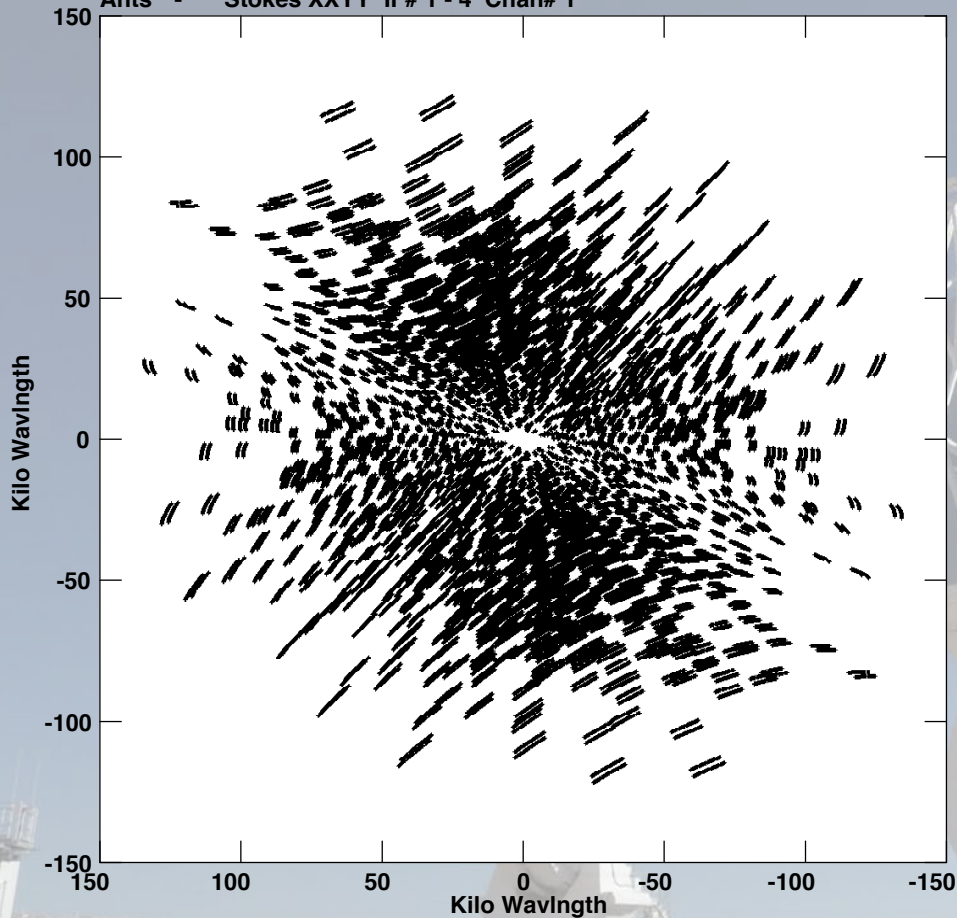
17:20-17:32 UT (1 scan), spw 0~3,  
12m array

“Dirty beam”: rms ~ 1.4%



# ALMA Band 3

Plot file version 4 created 24-FEB-2020 13:27:39  
V vs U for SUN 3 MM.UVR12.1 Source:Sun\_10  
Ants \* - \* Stokes XXYY IF# 1 - 4 Chan# 1

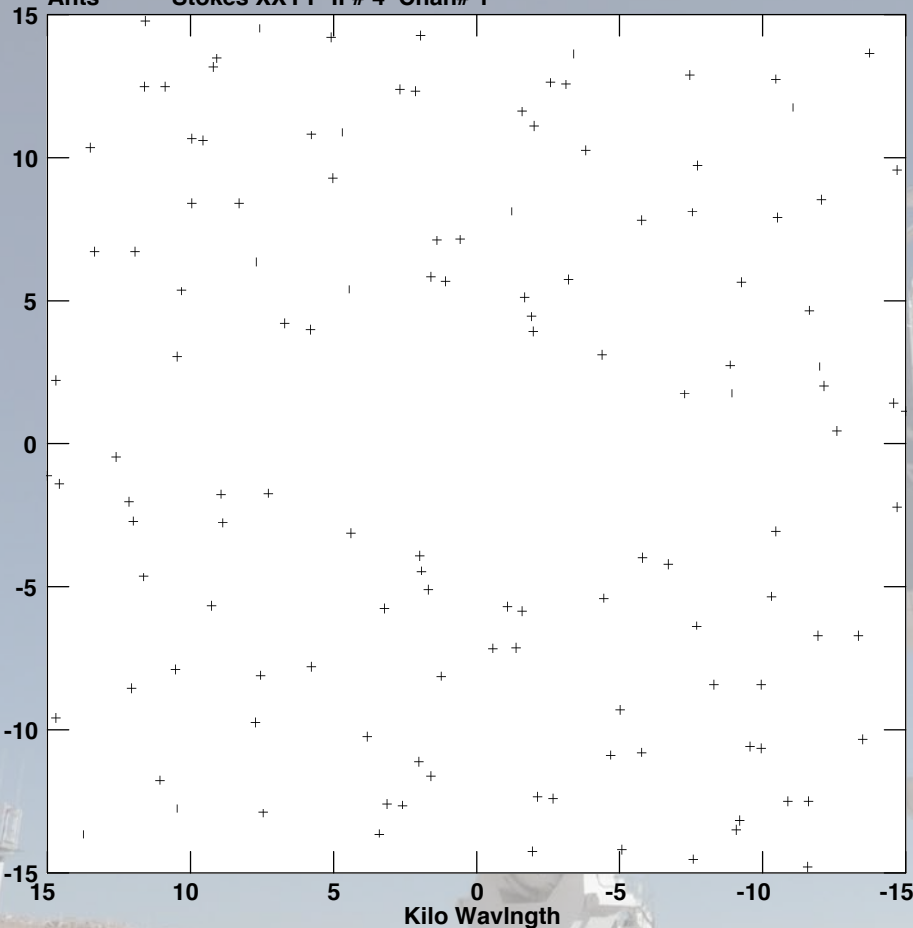


17:20-18:03 (4 scans), spw 0~3,  
12m array

“Dirty beam”: rms ~ 0.7%

# ALMA Band 3

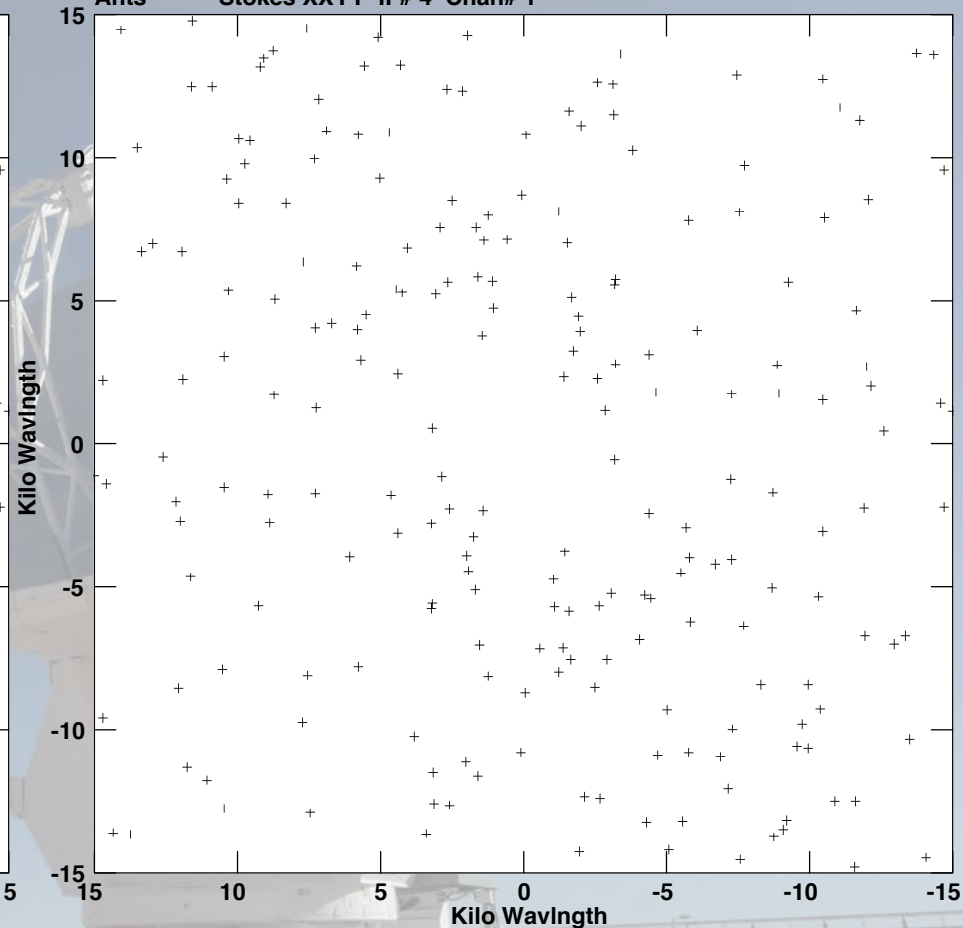
Plot file version 1 created 28-FEB-2020 10:55:38  
V vs U for SUN 3 MM.UVR12.1 Source:Sun\_10  
Ants \* - \* Stokes XXYY IF# 4 Chan# 1



From 0/17:25:00 to 0/17:25:02

2 s snapshot, spw 3, 12 m array

Plot file version 2 created 28-FEB-2020 10:55:44  
V vs U for SUN 3 MM.UVR12.1 Source:Sun\_10  
Ants \* - \* Stokes XXYY IF# 4 Chan# 1

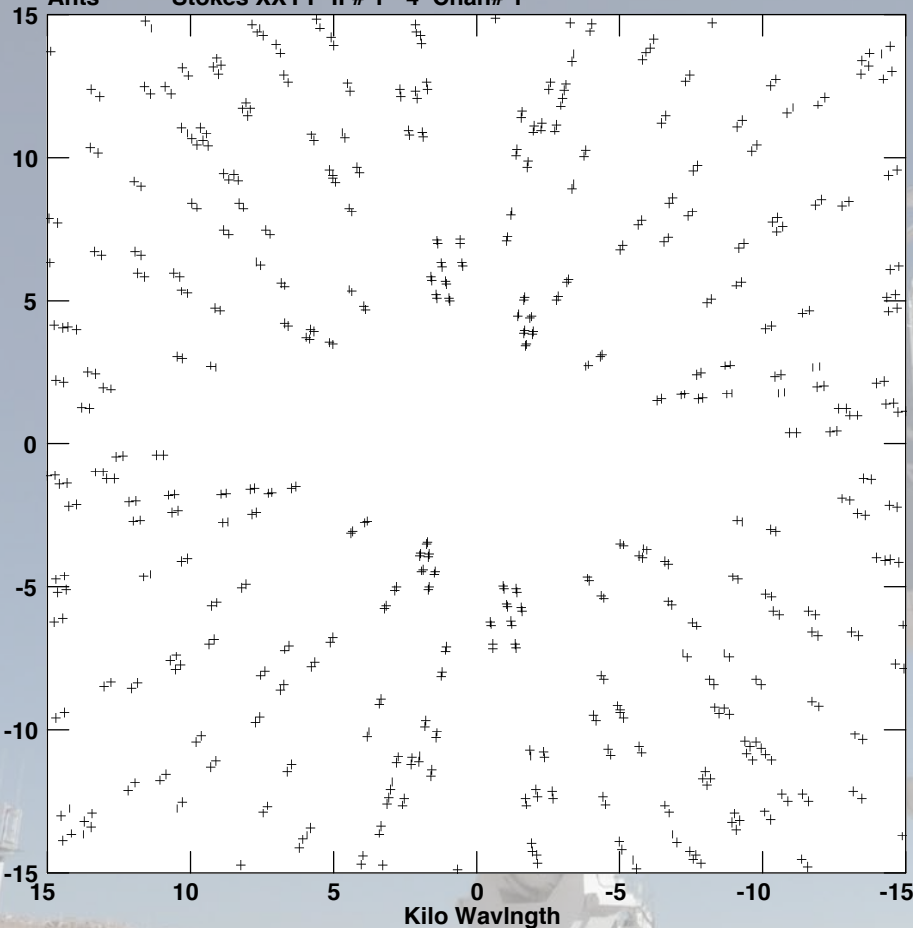


From 0/17:25:00 to 0/17:25:02

12 m array + ACA  
12m x 12m, 7m x 7m, & 7m x 12m

# ALMA Band 3

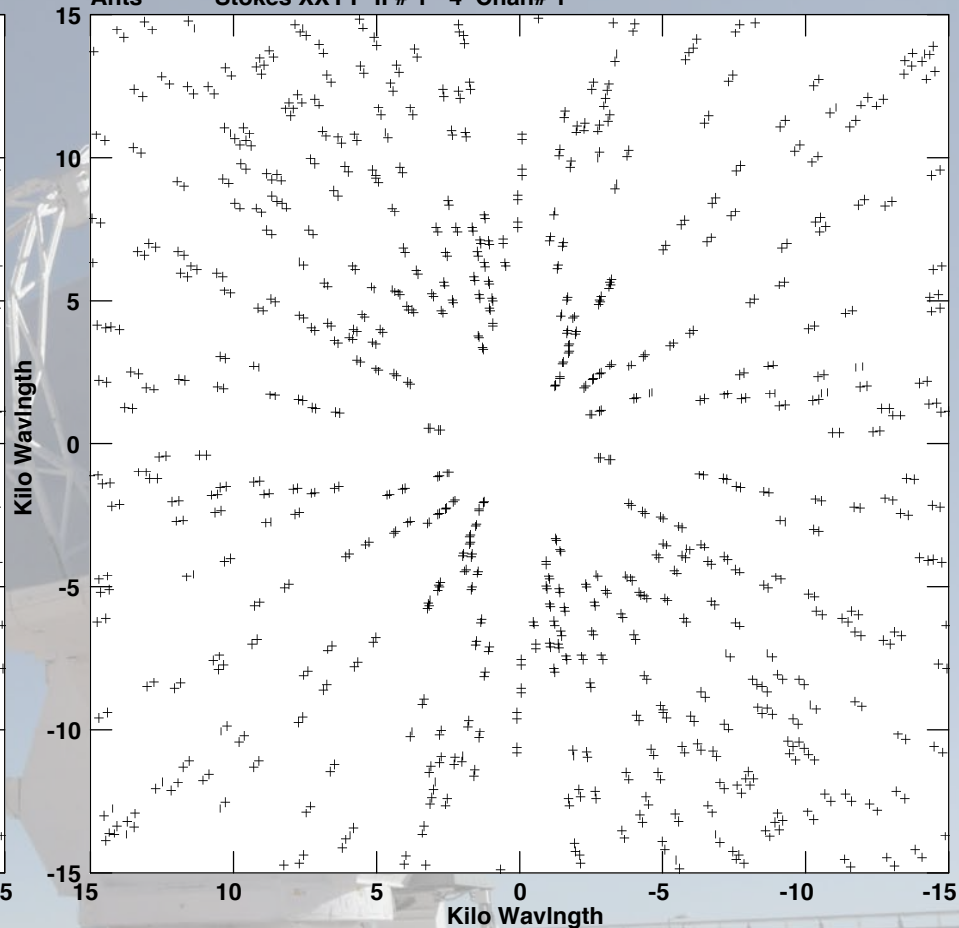
Plot file version 3 created 28-FEB-2020 10:55:51  
V vs U for SUN 3 MM.UVR12.1 Source:Sun\_10  
Ants \* - \* Stokes XXYY IF# 1 - 4 Chan# 1



From 0/17:25:00 to 0/17:25:02

2 s snapshot, spw 0~3, 12m array

Plot file version 4 created 28-FEB-2020 10:55:56  
V vs U for SUN 3 MM.UVR12.1 Source:Sun\_10  
Ants \* - \* Stokes XXYY IF# 1 - 4 Chan# 1



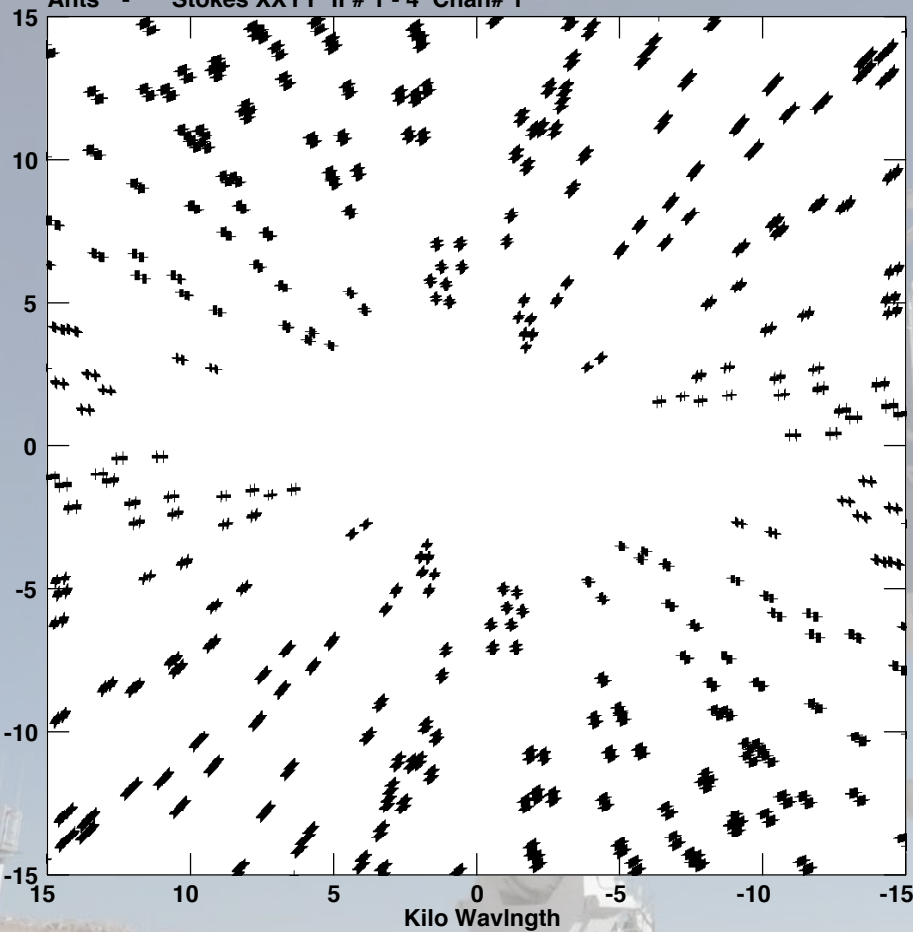
From 0/17:25:00 to 0/17:25:02

12 m array + ACA  
12m x 12m, 7m x 7m, & 7m x 12m



# ALMA Band 3

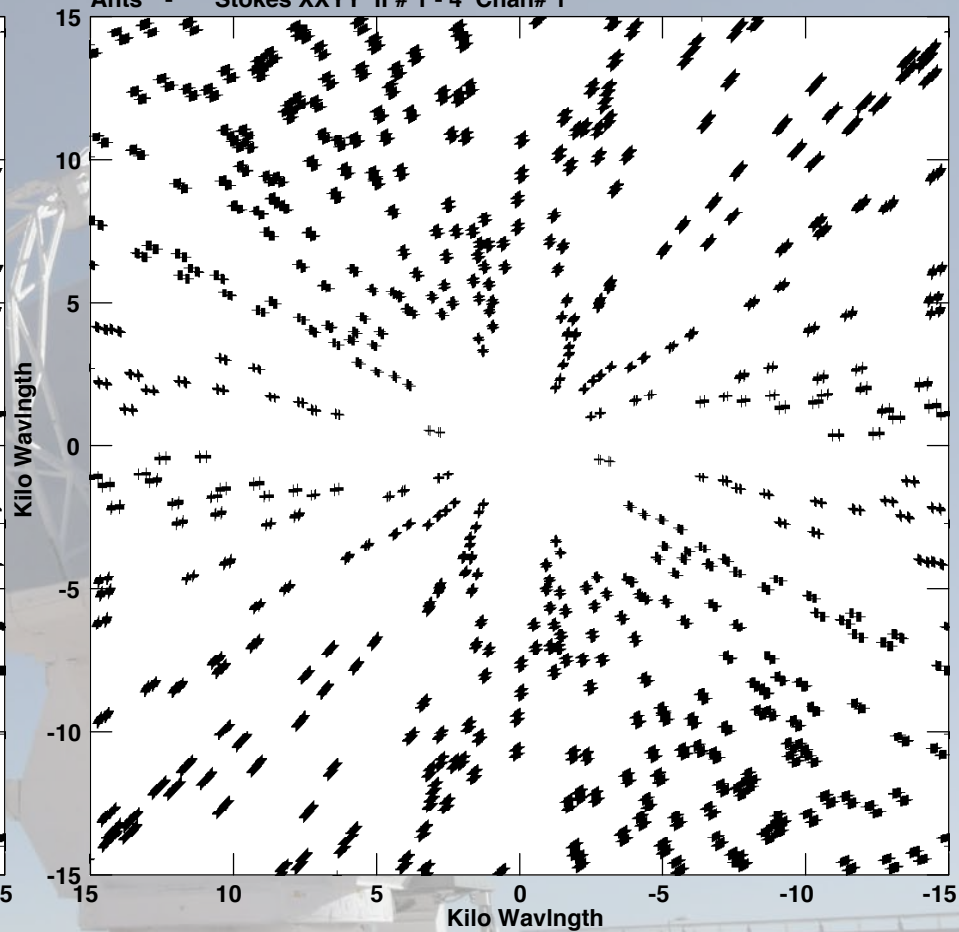
Plot file version 5 created 28-FEB-2020 10:56:24  
V vs U for SUN 3 MM.UVR12.1 Source:Sun\_10  
Ants \* - \* Stokes XXYY IF# 1 - 4 Chan# 1



From 0/00:00:00 to 0/17:32:00

17:20-17:32 UT (1 scan), spw 0~3,  
12m array

Plot file version 6 created 28-FEB-2020 10:56:29  
V vs U for SUN 3 MM.UVR12.1 Source:Sun\_10  
Ants \* - \* Stokes XXYY IF# 1 - 4 Chan# 1

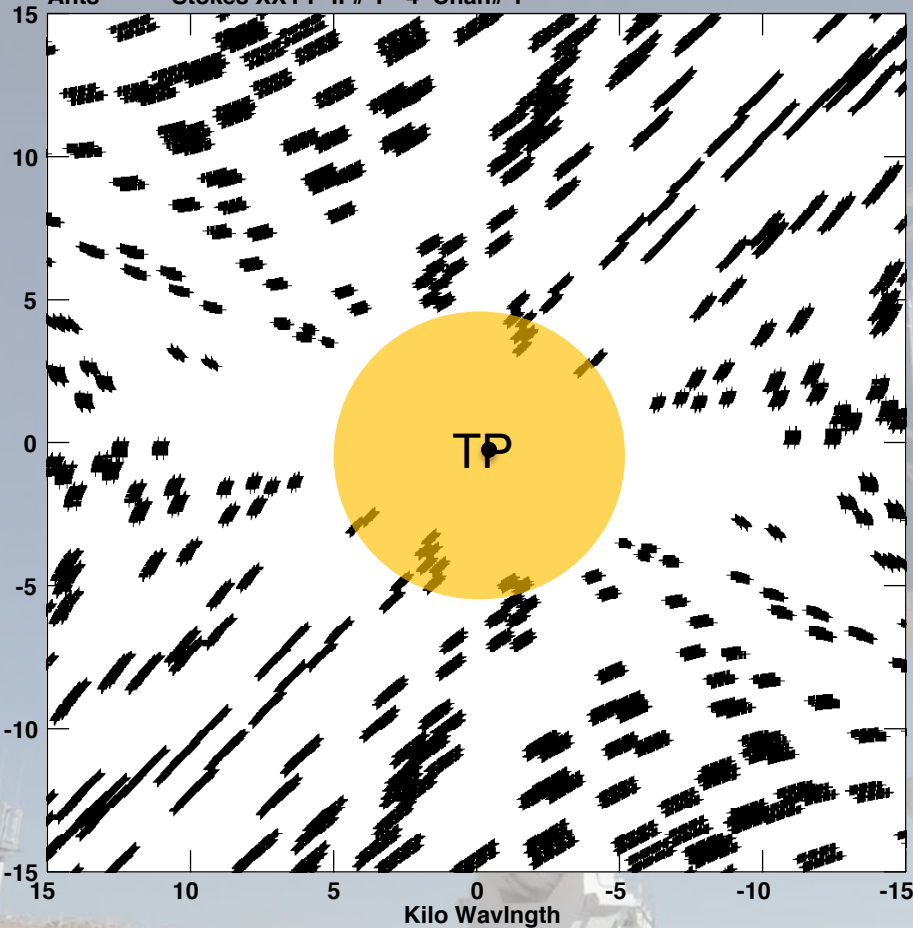


From 0/00:00:00 to 0/17:32:00

12 m array + ACA  
12m x 12m, 7m x 7m, & 7m x 12m

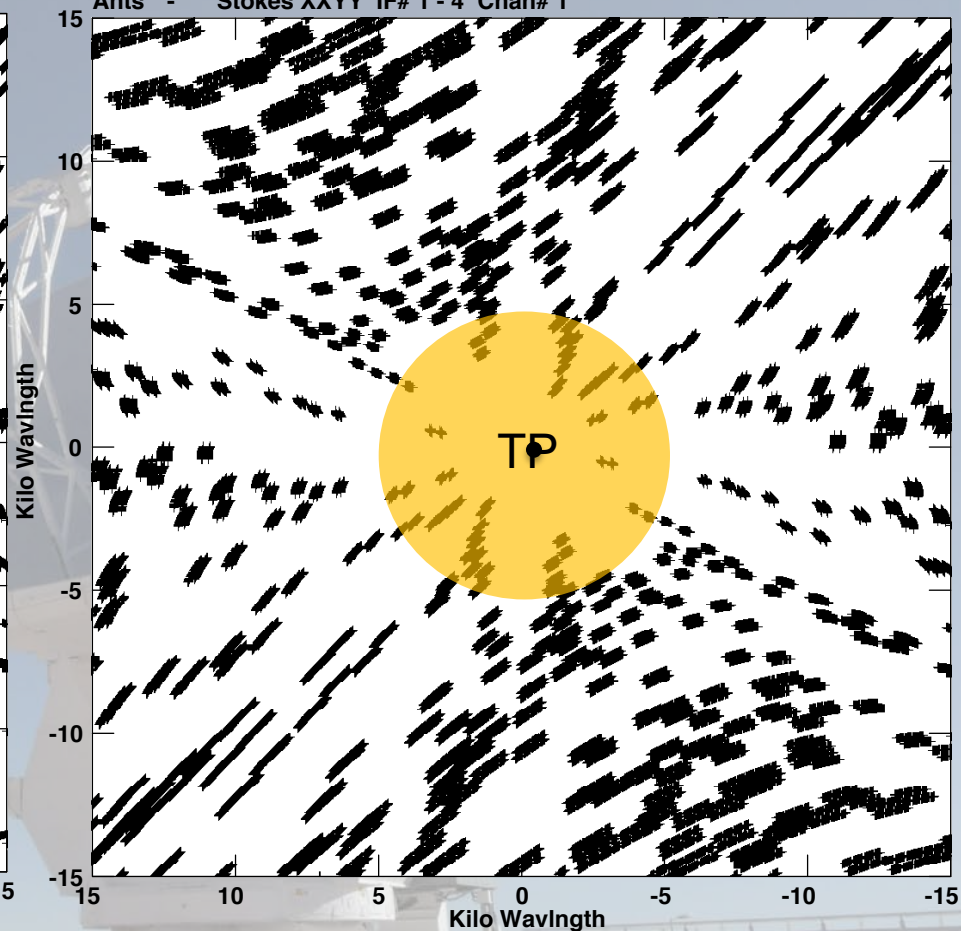
# ALMA Band 3

Plot file version 7 created 28-FEB-2020 10:56:38  
V vs U for SUN 3 MM.UVR12.1 Source:Sun\_10  
Ants \* - \* Stokes XXYY IF# 1 - 4 Chan# 1



17:20-18:03 (4 scans), spw 0~3,  
12m array

Plot file version 8 created 28-FEB-2020 10:56:44  
V vs U for SUN 3 MM.UVR12.1 Source:Sun\_10  
Ants \* - \* Stokes XXYY IF# 1 - 4 Chan# 1



12 m array + ACA  
12m x 12m, 7m x 7m, & 7m x 12m

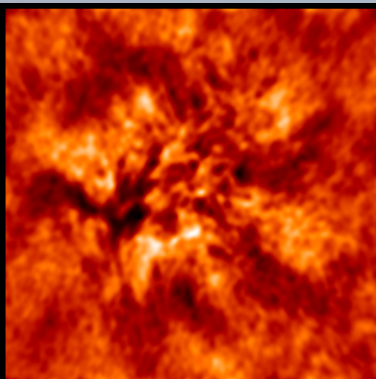
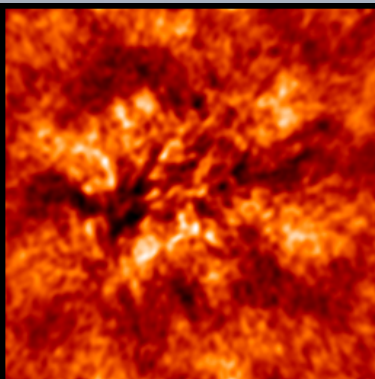
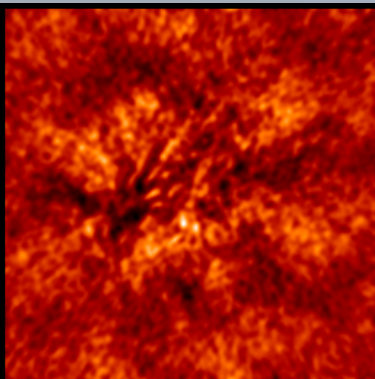
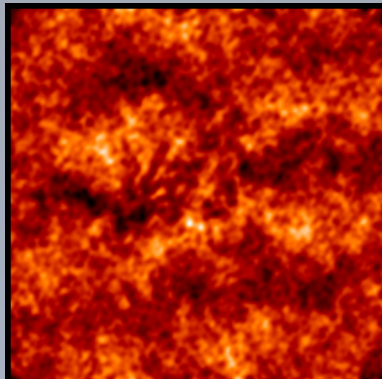
Snapshot (2s)  
spw 3

Snapshot (2s)  
spw 0-3

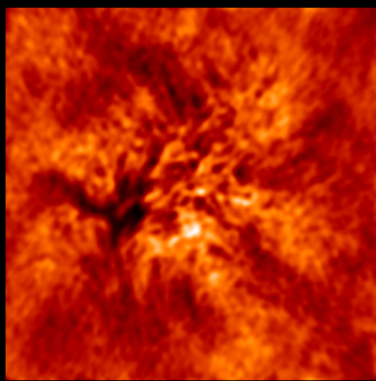
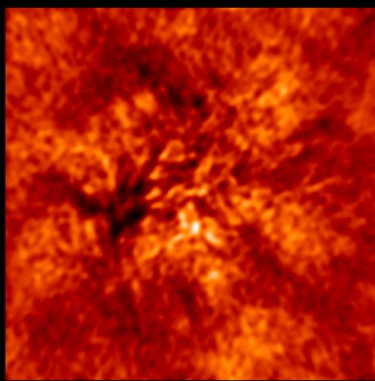
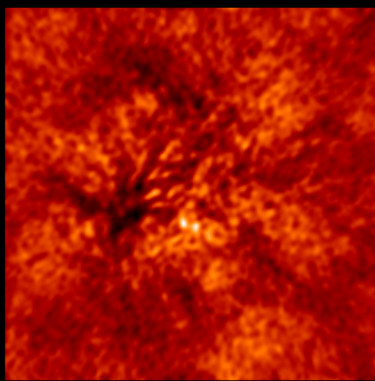
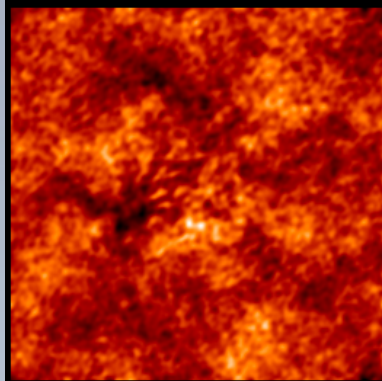
Scan (~10 min)  
spw 0-3

4 scans (~50 min)  
spw 0-3

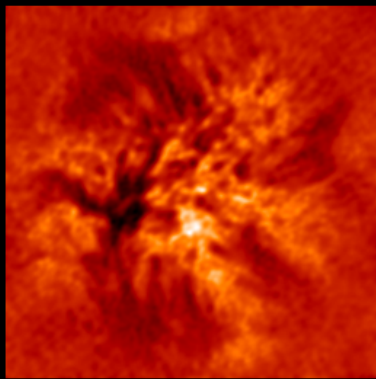
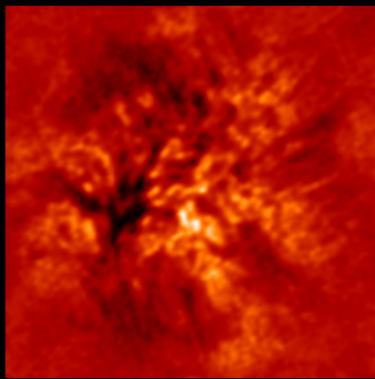
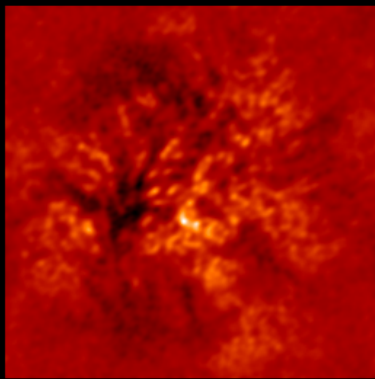
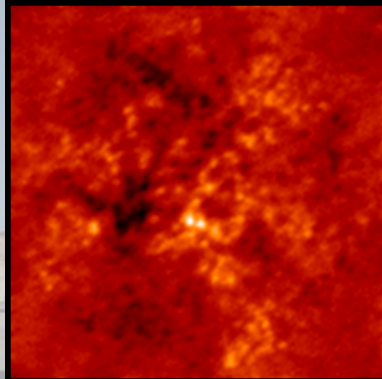
QA2  
dirty



SC  
dirty



Clean





# Visibility weighting

$$V^W(u, v) = \sum_{k=1}^M T_k D_k \delta(u - u_k, v - v_k) V'(u, v)$$

$$D_k \sim 1$$

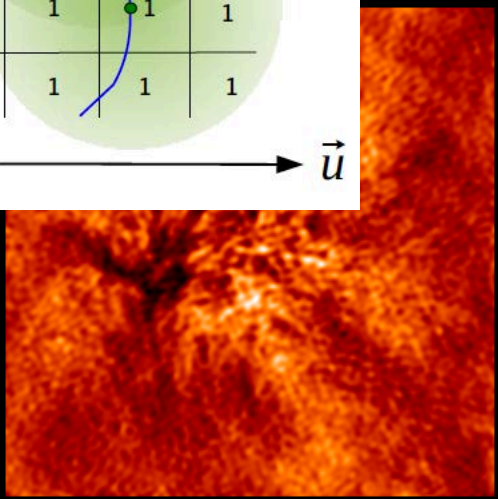
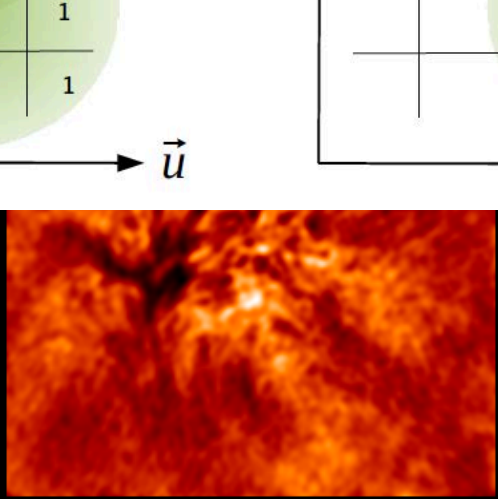
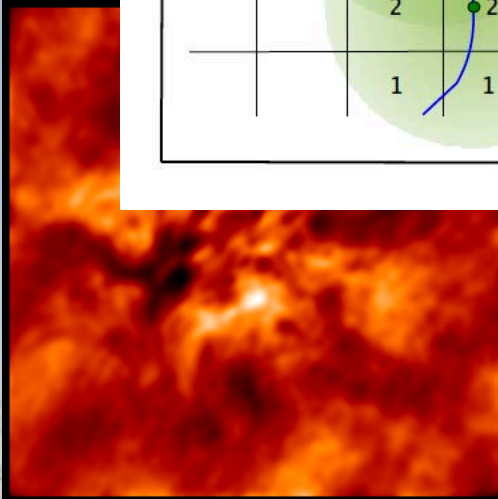
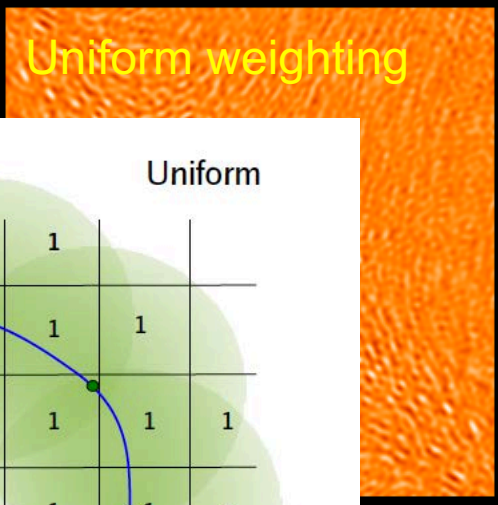
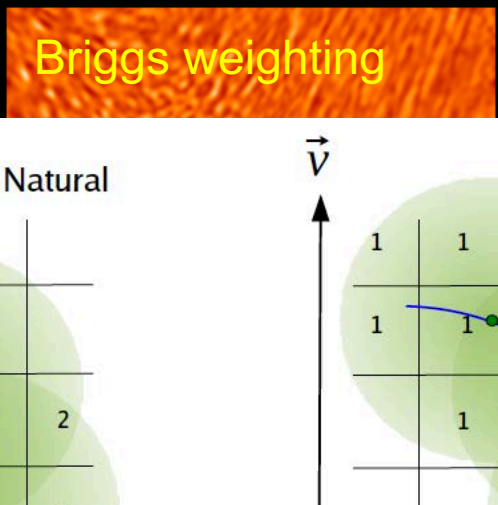
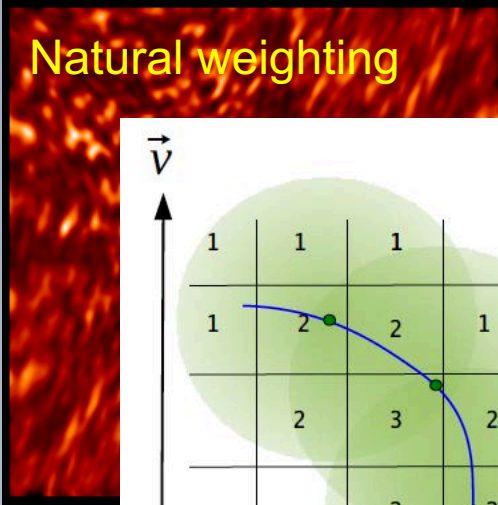
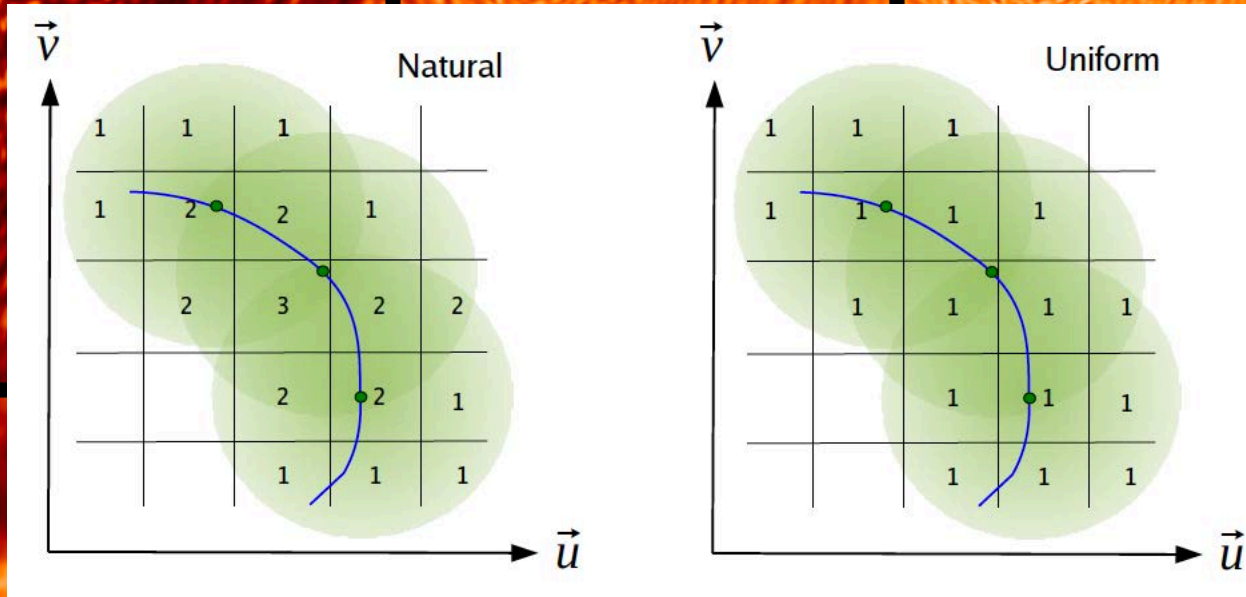
$$D_k \sim 1/(\alpha \rho_k + \sigma_k^2)$$

$$D_k \sim 1/\rho_k$$

Natural weighting

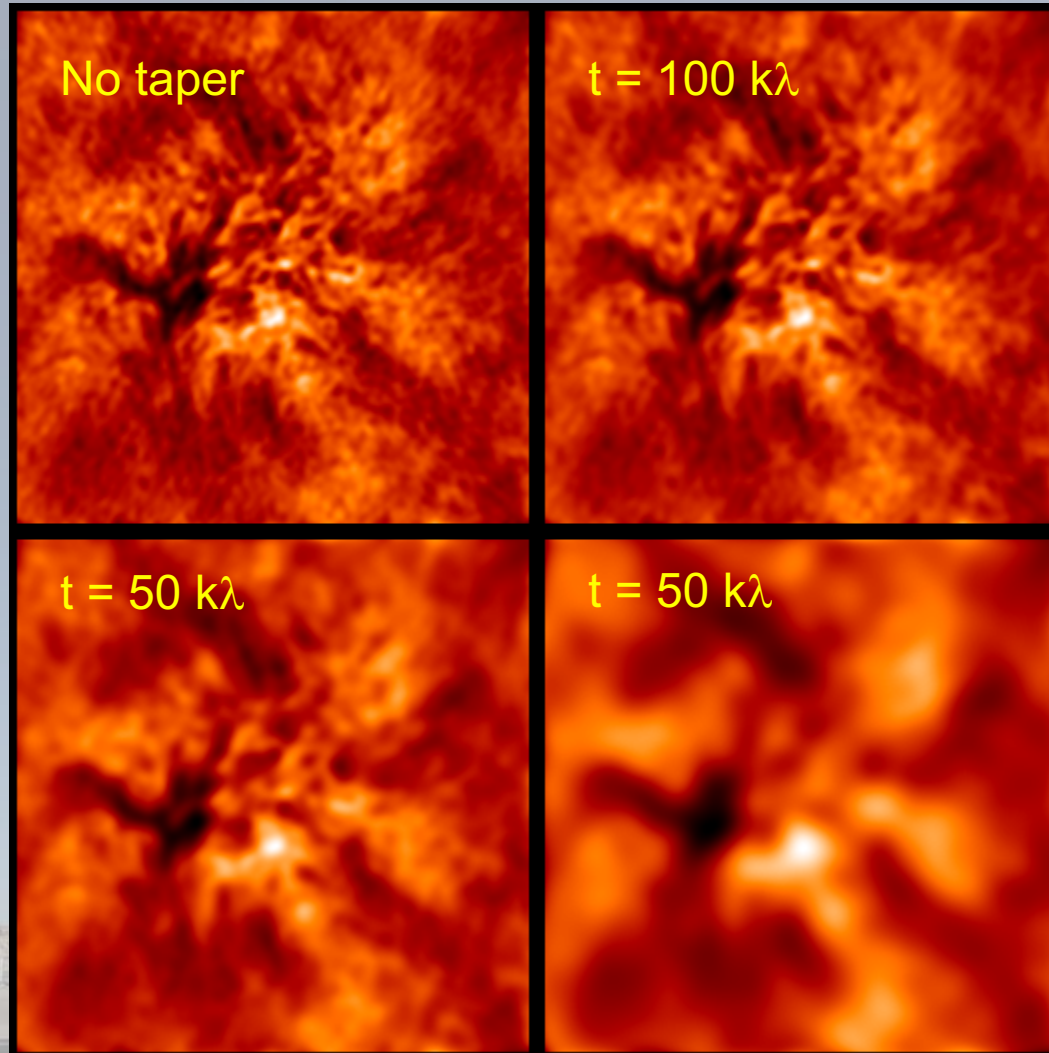
Briggs weighting

Uniform weighting



**Visibility weighting**  $V^W(u, v) = \sum_{k=1}^M T_k D_k \delta(u - u_k, v - v_k) V'(u, v)$

$$T_k = \exp[-(u^2 + v^2)/t^2]$$



# CLEAN bias

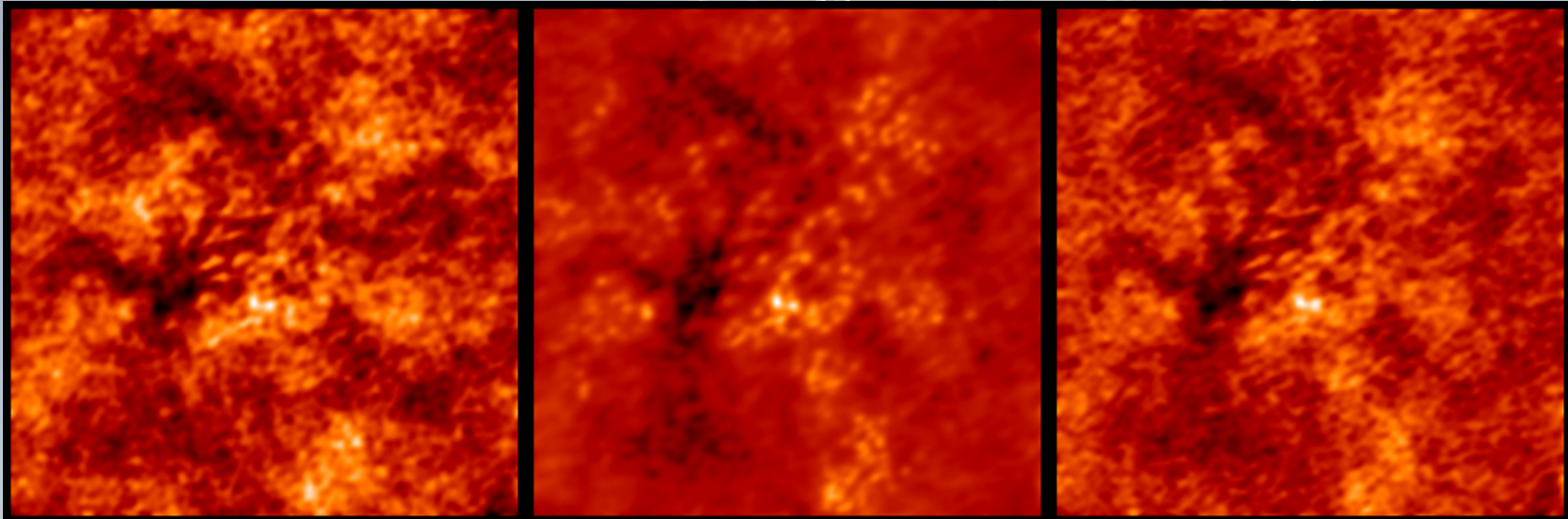
Well-known from VLA experience, particularly for snapshot imaging (e.g., surveys – see Condon et al. 1998).

CLEAN can misidentify sidelobe emission as source emission, particularly when the FOV is filled with complex emission.

"dirty" snapshot

CLEAN

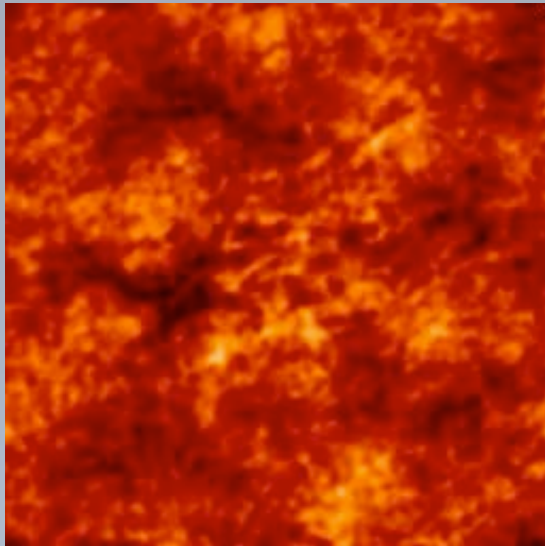
SDI CLEAN



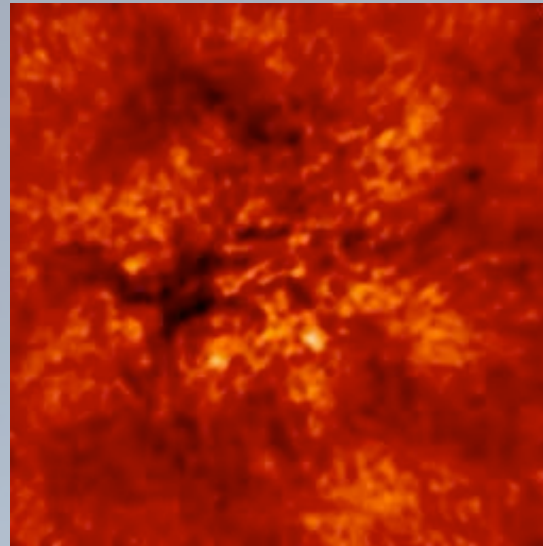


# Self-calibration example: Band 3

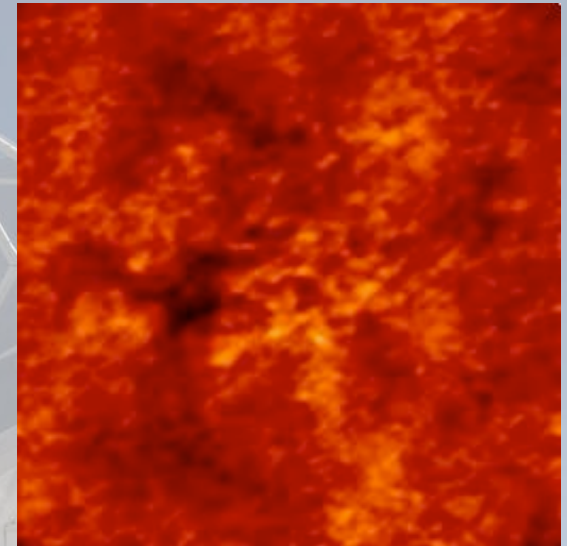
“dirty”, no S-C



“dirty”, S-C



SDI CLEAN, S-C



- Four iterations of self-cal in phase only, with diminishing integration time
- One iteration of both amplitude and phase self-cal
- Largest effects are to remove image wander and to improve effective angular resolution and SNR
- Use of SDI algorithm to avoid CLEAN artifacts and bias